

# Surface and bulk transitions in three-dimensional $O(n)$ models

Youjin Deng <sup>1,2</sup>, Henk W.J. Blöte <sup>2,3</sup>, and M. P. Nightingale <sup>4</sup>

<sup>1</sup>*Laboratory for Materials Science, Delft University of Technology,*

*Rotterdamseweg 137, 2628 AL Delft, The Netherlands*

<sup>2</sup>*Faculty of Applied Sciences, Delft University of Technology,*

*P.O. Box 5046, 2600 GA Delft, The Netherlands*

<sup>3</sup>*Lorentz Institute, Leiden University, P.O. Box 9506,*

*2300 RA Leiden, The Netherlands and*

<sup>4</sup>*Department of Physics, University of Rhode Island, Kingston, Rhode Island 02881, USA*

Using Monte Carlo methods and finite-size scaling, we investigate surface criticality in the  $O(n)$  models on the simple-cubic lattice with  $n = 1, 2$ , and  $3$ , i.e. the Ising,  $XY$ , and Heisenberg models. For the critical couplings we find  $K_c(n = 2) = 0.4541655(10)$  and  $K_c(n = 3) = 0.693002(2)$ . We simulate the three models with open surfaces and determine the surface magnetic exponents at the ordinary transition to be  $y_{h1}^{(o)} = 0.7374(15)$ ,  $0.781(2)$ , and  $0.813(2)$  for  $n = 1, 2$ , and  $3$ , respectively. Then we vary the surface coupling  $K_1$  and locate the so-called special transition at  $\kappa_c(n = 1) = 0.50214(8)$  and  $\kappa_c(n = 2) = 0.6222(3)$ , where  $\kappa = K_1/K - 1$ . The corresponding surface thermal and magnetic exponents are  $y_{t1}^{(s)} = 0.715(1)$  and  $y_{h1}^{(s)} = 1.636(1)$  for the Ising model, and  $y_{t1}^{(s)} = 0.608(4)$  and  $y_{h1}^{(s)} = 1.675(1)$  for the  $XY$  model. Finite-size corrections with an exponent close to  $-1/2$  occur for both models. Also for the Heisenberg model we find substantial evidence for the existence of a special surface transition.

PACS numbers: 05.50.+q, 64.60.Cn, 64.60.Fr, 75.10.Hk

## I. INTRODUCTION

In the past decades, surface effects near a phase transition have been investigated extensively, and many results have been obtained by means of mean-field theory, series expansions, renormalization and field-theoretic analyses. For reviews, see e.g. Refs. 1,2, and for more recent work see Refs. 3,4. In particular, at a second-order phase transition, where long-range correlations emerge, surface effects can be significant. The surfaces display critical phenom-

ena which differ from the bulk critical behavior; several surface universality classes can exist for one bulk universality class. We shall refer to the various types of transitions using the terminology of Ref. 1.

In this work, we investigate surface critical phenomena in three-dimensional  $O(n)$  models, namely the Ising ( $n = 1$ ), the  $XY$  ( $n = 2$ ), and the Heisenberg ( $n = 3$ ) model. The reduced Hamiltonian of these models can be written as the sum of two parts: a bulk term proportional to the volume of the system and a surface term proportional to the surface area, i.e.,

$$\mathcal{H}/k_B T = -K \sum_{\langle ij \rangle}^{(b)} \vec{s}_i \cdot \vec{s}_j - \vec{H} \cdot \sum_k^{(b)} \vec{s}_k - K_1 \sum_{\langle pq \rangle}^{(s)} \vec{s}_p \cdot \vec{s}_q - \vec{H}_1 \cdot \sum_r^{(s)} \vec{s}_r, \quad (1)$$

where the dynamic variable  $\vec{s}$  is a unit vector of  $n$  components. The parameters  $K$  and  $K_1$  are the strenghts of the coupling between nearest-neighbor sites in the bulk and on the surface layers, respectively, and  $H$  and  $H_1$  represent the reduced magnetic fields. The first two sums in Eq. (1) account for the bulk and the last two sums involve the spins on the open surfaces. For ferromagnetic bulk and surface couplings ( $K > 0$  and  $K_1 > 0$ ), the phase transitions are sketched in Fig. 1 for the case of the Ising and the  $XY$  model. In the high-temperature region, i.e., for bulk coupling  $K < K_c$ , the bulk is in the paramagnetic state, so that the bulk correlation length remains finite. However, a phase transition can still occur on the open surface when the surface coupling  $K_1$  is sufficiently enhanced. This phase transition is referred to as the “surface transition,” and is represented by the solid curve in Fig. 1. These phase transitions are generally thought to be in the same universality classes as the two-dimensional Ising and the  $XY$  model, respectively. At the bulk critical point  $K = K_c$ , the line of surface phase transitions terminates at a point  $(K_c, K_{1c})$ . At this point, both the surface and the bulk correlation length diverge. Thus, the point  $(K_c, K_{1c})$  acts as a multicritical point, and the phase transition is referred to as the “special transition.” For  $K_1 < K_{1c}$ , the bulk and the surfaces simultaneously undergo a phase transition at  $K = K_c$ . In this case, the critical correlations on the surfaces arise from the diverging bulk correlation lengths, and the transition is named the “ordinary transition.” The ordinary transition remains within the same universality class for a wide range of surface couplings. The correlation functions on and near the surface appear to fit universal profiles<sup>5</sup>. The transitions at  $K = K_c$  for  $K_1 > K_{1c}$  are referred to as the “extraordinary transitions.” For the Ising model, since the surfaces are already in the ferromagnetic state for a smaller coupling  $K < K_c$ , no surface transition occurs when the bulk critical line  $K = K_c$  is crossed.

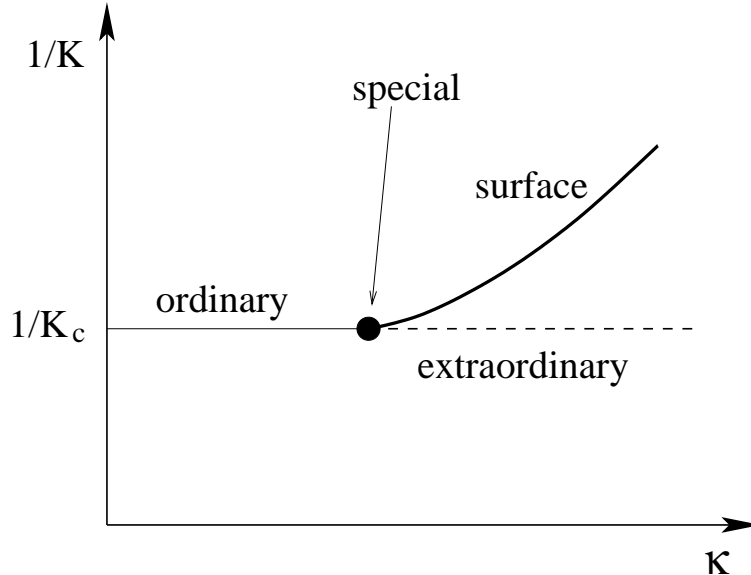


FIG. 1: Sketch of the surface phase transitions of the three-dimensional Ising and  $XY$  models with ferromagnetic couplings. The vertical axis is the bulk temperature  $1/K$ , and the parameter  $\kappa = (K_1 - K)/K$  in the horizontal axis represents the enhancement of the surface couplings. The “surface,” the “ordinary,” and the “extraordinary” phase transitions are represented by the thick solid, the thin solid, and the dashed line, respectively. The lines meet in a point, shown as the black circle, which is referred to as the “special” phase transition.

Nevertheless, owing to the diverging bulk correlation length, the surfaces still display critical correlations at  $K = K_c$ . For the  $XY$  model, however, the surface transitions for  $K < K_c$  are Kosterlitz-Thouless-like<sup>6</sup>, i.e., the surfaces do not display long-range order for  $K < K_c$ , in agreement with results of Landau and co-workers<sup>7</sup>.

For three-dimensional  $O(n)$  models with  $n > 2$ , which include the Heisenberg model, the line of surface transitions for  $K < K_c$  does not exist; it may thus seem self-evident that the special and the extraordinary transitions are also absent. However, this remains to be investigated; for instance, in two-dimensional tricritical Potts models, a line of edge transitions is absent, but special and extraordinary transitions do exist<sup>8</sup>. Thus, even without a line of surface transitions for  $K < K_c$ , rich surface critical phenomena can still occur in the three-dimensional Heisenberg model. For instance, it was reported<sup>9</sup> that at bulk criticality  $K = K_c$  the surface magnetic exponents depend on the ratio  $K_1/K$  for  $K_1/K \geq 2.0$ . This brings up the question whether

Additional surface critical phenomena can occur for the Ising model, if the surface and/or the bulk couplings are allowed to be antiferromagnetic. Further, one can allow the spins on the surface to vanish, such that the surface part of the Hamiltonian in Eq. (1) is described by the so-called Blume-Capel model. Such spin-0 states act as annealed vacancies on the surfaces. It was observed<sup>10</sup> that, by varying the fugacity of the vacancies, one can reach a point where the bulk Ising criticality  $K = K_c$  joins the line of surface transitions that belongs to the universality class of the two-dimensional tricritical Ising model. This point was named<sup>10</sup> the “tricritical special” phase transition. In short, for each bulk universality class, surface transitions in various surface universality classes can occur, including the ordinary, special, and extraordinary transitions at  $K = K_c$ , and the surface transitions at  $K < K_c$ .

Apart from the bulk renormalization exponents, additional surface exponents are needed to describe the above surface critical behavior. At the ordinary and the extraordinary transitions, the surface magnetic scaling field is relevant, while the surface thermal field is irrelevant. At the special transition, both the magnetic and the thermal surface fields are relevant.

Since exact information about critical behavior is scarce in three dimensions, determinations of these surface critical exponents rely on approximations of various kinds. These include mean-field theory<sup>1,11,12,13</sup>, series expansions<sup>14</sup>, renormalization group technique<sup>2,3,15,16,17</sup>, Monte Carlo simulations<sup>5,7,18,19,20,21,22</sup>, etc.

The surface critical index  $\beta_1$  is defined so as to describe the asymptotic scaling behavior of the surface magnetization  $m_1$  as a function of the bulk thermal field  $t$ , i.e.,  $m_1 \propto t^{\beta_1}$ . From the scaling relations it follows that this exponent is related to the critical exponents as  $\beta_1 = (d - 1 - y_{h1})/y_t$ , where  $y_t$  and  $y_{h1}$  are the bulk thermal and the surface magnetic exponent, respectively, and  $d = 3$  is the spatial dimensionality. The mean-field analysis and the Gaussian fixed point of the  $\phi^4$  theory yield the magnetic surface index  $\beta_1$  as  $\beta_1^{(o)} = 1$ ,  $\beta_1^{(s)} = 1/2$ , and  $\beta_1^{(e)} = 1$  respectively for the ordinary, special, and extraordinary transition. Many numerical results also exist. For the simple-cubic lattice, the special transition of the Ising model was located as  $\kappa_c = 0.5004(2)$ <sup>19,20</sup>. Although the values of critical couplings  $K_c$  and  $K_{1c}$  are far from the mean-field predictions, the above result for  $\kappa_c$  is in agreement with the mean-field value  $\kappa_c = 1/2$ . Further, the surface critical exponents are determined<sup>19,20,21,23</sup> as  $y_{h1}^{(o)} = 0.737(5)$ ,  $y_{h1}^{(s)} = 1.62(2)$ , and  $y_{t1}^{(s)} = 0.94(6)$ . Compared to the Ising model,

there are fewer investigations for the three-dimensional  $XY$  and the Heisenberg model. In particular, to our knowledge, numerical determinations of the special transition and the corresponding surface critical exponents have not yet been reported for the  $XY$  model. Most of the existing results for the Ising, the  $XY$  and the Heisenberg model will be tabulated below, together with new results of the present work.

The present work aims to provide an extensive and systematic Monte Carlo investigation of the phase transitions of the surfaces of the three-dimensional Ising,  $XY$ , and Heisenberg models. Compared to numerical investigations one or two decades ago, one has the following advantages. Firstly, the bulk critical points of these systems have now been determined accurately. On the simple cubic lattice, the bulk critical point of the Ising model was determined as  $K_c(n=1) = 0.221\,654\,55(3)^{24}$ , with the uncertainty only in the eighth decimal place. The bulk transitions of the  $XY$  and the Heisenberg model were also determined<sup>14,25,26,27,28,29,30</sup> to occur at  $K_c = 0.454\,167(4)$  and  $0.693\,002(12)$ , respectively. In the present paper, we also simulate these two systems with periodic boundary conditions, and improve the above estimations as  $K_c(n=2) = 0.454\,1655(10)$  and  $K_c(n=3) = 0.693\,002(2)$ . Secondly, the rapid development of computer technology makes it possible to perform extensive computations at a limited cost. The present work was performed on 20 PCs; the total computer time is in the order of 20 CPU months at a processor speed of 2.5 GHz.

The organization of the present paper is as follows. Section II reviews the finite-size-scaling properties of the systems defined by Eq. (1), with the emphasis on the sampled quantities required for the numerical analysis of the simulation data. Section III describes the determination of the critical points of the  $XY$  and Heisenberg models. Sections IV, V, and VI present the Monte Carlo simulations and the results for the Ising,  $XY$ , and Heisenberg models, respectively. Section VII concludes the paper with a brief discussion.

## II. FINITE-SIZE SCALING AND SAMPLED QUANTITIES

The total free energy of a system with free surfaces can, in analogy with the Hamiltonian in Eq. (1), be expressed as the sum of a bulk and a surface term<sup>1,31,32</sup>:

$$F = f_b V + f_1 S , \quad (2)$$

where  $f_b$  and  $f_1$  are the densities of the bulk and the surface parts of the free energy, respectively, and  $V$  and  $S$  represent the total volume and the surface area, respectively. Near criticality, the finite-size scaling behavior of  $f_b$  and  $f_1$  is given by the equations

$$f_b(t, h, L) = L^{-d} f_{bs}(tL^{y_t}, hL^{y_h}) + f_{ba}(t, h), \quad (3)$$

and

$$f_1(t, h, t_1, h_1, L) = L^{-(d-1)} f_{1s}(tL^{y_t}, hL^{y_h}, t_1L^{y_{t_1}}, h_1L^{y_{h_1}}) + f_{1a}(t, h, t_1, h_1). \quad (4)$$

The functions  $f_{bs}$  and  $f_{ba}$  are the singular and the analytical parts of  $f_b$ ;  $f_{1s}$  and  $f_{1a}$  similarly apply to the surface free-energy density  $f_1$ . The bulk thermal and magnetic scaling fields are represented by  $t$  and  $h$ , and the surface scaling fields by  $t_1$  and  $h_1$ . The associated exponents are labeled with corresponding subscripts. As implied by Eq. (3), the leading scaling behavior of the bulk does not depend on the presence of free surfaces, although physical quantities near the surfaces can be significantly affected.

On the basis of Eqs. (3) and (4), the scaling behavior of various quantities can be obtained as derivatives of  $f_b$  and  $f_s$  with respect to the appropriate scaling fields. Details can be found in Ref. 1.

The determination of the bulk critical points used simulations of  $L \times L \times L$  with periodic boundary conditions in which case  $f_1$  vanishes. The sampling procedure involved the determination of the bulk magnetization density

$$\vec{m} \equiv N^{-1} \sum_{k=1}^N \vec{s}_k, \quad (5)$$

where  $N = L^3$ . This yielded the averages of the magnetization moments  $\langle \vec{m} \cdot \vec{m} \rangle$  and  $\langle (\vec{m} \cdot \vec{m})^2 \rangle$ . The quantity

$$Q(K, L) \equiv \frac{\langle \vec{m} \cdot \vec{m} \rangle^2}{\langle (\vec{m} \cdot \vec{m})^2 \rangle}, \quad (6)$$

which is related to the Binder cumulant<sup>33</sup>, converges to a universal value  $Q$  at the critical point, and was used to determine the critical coupling  $K_c$ . The finite-size scaling behavior of  $Q$  can be found by writing the moments of  $\vec{m}$  in terms of derivatives of the free energy with respect to the magnetic field. After application of a scaling transformation, the singular powers in  $Q$  associated with field derivatives cancel, as do the powers of the nonuniversal metric factor relating the physical field and the magnetic scaling field. In the vicinity of

the critical point one obtains, in terms of the temperature scaling field  $t$  and an irrelevant temperature-like field  $u$ ,

$$Q(t, u, L) = \tilde{Q}(tL^{y_t}, uL^{y_i}) + b_2 L^{3-2y_h} + b_3 L^{y_t-2y_h} + \dots \quad (7)$$

where  $y_i$  is the leading irrelevant exponent. The correction term with amplitude  $b_2$  is due to the analytic contribution to the second moment of  $\vec{m}$ , and that with amplitude  $b_3$  to the second-order dependence of the temperature field on the physical magnetic field. Apart from corrections, the temperature field is proportional to  $K - K_c$ . Eq. (7) will be used in Sec. III to determine the bulk critical points.

In order to investigate surface critical behavior, we simulated  $L \times L \times L$  simple-cubic lattices with periodic boundary conditions in the  $xy$  plane and free boundaries in the  $z$  direction. First, we sampled the components of the surface magnetization and obtained two generalized surface susceptibilities:

$$\chi_{11} = \frac{L^2}{2} \langle \vec{m}_1 \cdot \vec{m}_1 + \vec{m}_2 \cdot \vec{m}_2 \rangle, \quad \text{and} \quad \chi_{12} = L^2 \langle \vec{m}_1 \cdot \vec{m}_2 \rangle \quad (8)$$

where  $\vec{m}_1$  and  $\vec{m}_2$  are the magnetization densities at the free surfaces with  $z = 1$  and  $z = L$ , respectively. By differentiating the surface free energy with respect to magnetic fields that act on either one of the free surfaces, one finds that the singular parts of these surface susceptibilities scale as  $L^{2y_{h1}-2}$ .

In addition, we computed two surface-surface correlations

$$g_{11} = \frac{1}{2L^2} \sum_{x,y=1}^L (\langle \vec{s}_{x,y,1} \cdot \vec{s}_{x+r,y+r,1} + \vec{s}_{x,y,L} \cdot \vec{s}_{x+r,y+r,L} \rangle) \quad (r = L/2), \quad (9)$$

and

$$g_{12} = \frac{1}{L^2} \sum_{x,y=1}^L \langle \vec{s}_{x,y,1} \cdot \vec{s}_{x,y,L} \rangle. \quad (10)$$

Further, we sampled two ratios of surface magnetization moments:

$$Q_{11} = \frac{\langle \vec{m}_1 \cdot \vec{m}_1 \rangle^2}{\langle (\vec{m}_1 \cdot \vec{m}_1)^2 \rangle} \quad \text{and} \quad Q_{12} = \frac{\langle \vec{m}_1 \cdot \vec{m}_2 \rangle^2}{\langle (\vec{m}_1 \cdot \vec{m}_2)^2 \rangle}. \quad (11)$$

These quantities are the surface analogs of the bulk ratio  $Q$ , cf. Eq. (7), and will be used to locate the surface transitions.

TABLE I: Description of the simulations of the  $XY$  and Heisenberg models. The table lists the simulation length in millions of cycles ( $\#MC$ ), and the number of Wolff clusters ( $\#Wc/C$ ) per cycle, for each system size  $L$ . The data were taken range  $\Delta K$  of the coupling  $K$ . The values shown are those for the  $XY$  model; those for the Heisenberg model are approximately the same.

$L$	$\#MC$	$\#Wc/C$	$\Delta K$
4	50	2	0
6	50	3	0.016
8	50	4	0
10	20	5	0
12	20	6	0
14	20	7	0
16	80	8	0.006
20	20	10	0
24	20	12	0
28	20	14	0
32	80	16	0.002
40	20	20	0
48	20	24	0
64	20	32	0
96	15	48	0
160	6.7	80	0

### III. CRITICAL POINTS OF THE $O(2)$ AND THE $O(3)$ MODELS

The critical point of the Ising model on the simple cubic lattice is already known<sup>24</sup> with sufficient accuracy for the present purposes. We therefore restrict ourselves to the  $XY$  and Heisenberg models. We used the Wolff cluster algorithm<sup>34,35</sup> to simulate these models on simple-cubic lattices with periodic boundary conditions. Each cluster is constructed on the basis of one component of the spin vectors. The cluster formation process is thus very similar to that for the Ising model. Each simulation consists of a large number of cycles, each of



which contains several Wolff steps and a data sampling procedure. The Wolff cluster flips do not change the absolute values of the spin components. Thus, to satisfy ergodicity, each cycle also includes a random rotation of the whole system of spin vectors. We simulated a number of  $L^3$  systems whose finite sizes  $L$  are listed in Table I, together with the number of Wolff clusters per cycle and the total number of cycles per system size.

Most simulations of the  $XY$  model took place at  $K = 0.454\,15$ , and of the Heisenberg model at  $K = 0.693$ . Both values are already very close to the final estimates that we shall report for the respective critical points. To avoid bias effects associated with short binary shift registers<sup>36,37</sup> we took two such shift registers, with lengths equal to the Mersenne exponents 127 and 9689, and added the resulting two maximum-length bit sequences modulo 2. This procedure leads to a sequence whose leading deviation from randomness is a 9-bit correlation, which is a considerable improvement in comparison with the usual 3-bit correlations<sup>38</sup>.

The simulations yielded data for the Binder cumulant as described in the preceding Section. Expanding  $\tilde{Q}$  in Eq. (7) and expressing the temperature deviation from the critical point in  $K - K_c$ , leads to

$$Q(K, L) = Q + a_1(K - K_c)L^{y_t} + a_2(K - K_c)^2L^{2y_t} + \dots + b_1L^{y_i} + b_2L^{3-2y_h} + b_3L^{y_t-2y_h} + \dots \quad (12)$$

where  $Q$  is a universal constant and the correction term with amplitude  $b_1$  is due to the irrelevant field. This expression was used to analyze the numerical data for  $Q(K, L)$  by means of least-squares fits. The exponents were set to the estimates obtained by Guida and Zinn-Justin<sup>39</sup>, namely  $y_t = 1.492$ ,  $y_i = -0.789$  and  $y_h = 2.482$  for the  $XY$  model, and  $y_t = 1.414$ ,  $y_i = -0.782$  and  $y_h = 2.482$  for the Heisenberg model. In order to determine the amplitudes  $a_1$  and  $a_2$  we included some data for relatively small ( $L = 8, 16$  and  $32$ ) systems, taken at values of  $K$  differing up to the order of one percent from  $K_c$ . Satisfactory fits, as judged from the residual  $\chi^2$  compared with the number of degrees of freedom, were obtained including all system sizes down to  $L = 4$  for the  $XY$  and  $L = 6$  for the Heisenberg model. We found that mixed terms proportional to  $(K - K_c)L^{y_i+y_t}$  were insignificant.

The results for the critical points are  $K_c = 0.454\,1655(10)$  for the  $XY$  model and  $K_c = 0.693\,002(2)$  for the Heisenberg model. The universal values of the amplitude ratios are  $Q = 0.8049(2)$  for the  $XY$  model and  $Q = 0.8776(2)$  for the Heisenberg model. We obtained similar results with other types of fits, which involved fewer correction terms and

TABLE II: Summary of recent results for the critical coupling  $K_c$  of the three-dimensional  $XY$  and Heisenberg models on the simple-cubic lattice with nearest-neighbor interactions. The error margin in the last decimal place is shown in parentheses.

Reference	model	Year	$K_c$	
Janke <sup>40</sup>	O(2)	1993	0.454 08	(8)
Adler et al. <sup>28</sup>	O(2)	1993	0.454 14	(7)
Gottlob and Hasenbusch <sup>41</sup>	O(2)	1993	0.454 20	(2)
Butera and Comi <sup>42</sup>	O(2)	1997	0.454 19	(3)
Ballesteros et. al <sup>30</sup>	O(2)	1996	0.454 165	(4)
Cucchieri et. al <sup>29</sup>	O(2)	2002	0.454 167	(4)
Present work	O(2)	2004	0.454 1655	(10)
Chen et al. <sup>43</sup>	O(3)	1993	0.693 035	(37)
Holm and Janke <sup>44</sup>	O(3)	1993	0.693 0	(1)
Butera and Comi <sup>42</sup>	O(3)	1997	0.693 05	(4)
Ballesteros et al. <sup>30</sup>	O(3)	1996	0.693 002	(12)
Present work	O(3)	2004	0.693 002	(2)

excluded some of the smallest system sizes so as to obtain satisfactory residuals. This internal consistency confirms that our error estimates are realistic. The present results and some recent values taken from the literature are summarized in Table II.

#### IV. ISING MODEL

Although the three-dimensional Ising model has not been exactly solved, considerable information about its critical behavior is available from extensive investigations using various kinds of approximations. For a review see, e.g., Ref.<sup>45</sup>. For instance, evidence has been found that the Ising model is conformally invariant in three dimensions<sup>23,46</sup>. There is some consensus that the values of the bulk thermal and magnetic exponents,  $y_t$  and  $y_h$ , are 1.587 and 2.482, respectively, with uncertainty only in the last decimal place. The bulk critical points of a variety of three-dimensional systems with Ising universality have also been

obtained<sup>24</sup>; the bulk transition of the Ising model with nearest-neighbor interactions on the simple-cubic lattice was determined as  $K_c = 0.221\,654\,55\,(3)$ . The present work conveniently chooses this model so that no further work to determine  $K_c$  is required. As mentioned earlier, periodic boundary conditions are imposed in the  $xy$  plane and free boundaries along the  $z$  direction.

### A. Ordinary phase transition

Using the Wolff cluster algorithm<sup>34,35</sup>, we simulated the Ising model at bulk criticality, with the surface couplings chosen equal to the bulk couplings, i.e.,  $K_1 = K = K_c$ . The system sizes were taken as 16 even values in the range  $4 \leq L \leq 48$ . During the Monte Carlo simulations, we sampled the surface susceptibilities  $\chi_{11}$  and  $\chi_{12}$ , and the correlation functions  $g_{11}$  and  $g_{12}$ . To estimate  $y_{h1}^{(o)}$ , the universal surface magnetic exponent of the ordinary surface transition, we modeled the Monte Carlo data for the surface susceptibilities  $\chi_{11}$  and  $\chi_{12}$  by expressions of the form

$$\chi_1(L) = \chi_a + L^{2y_{h1}^{(o)}-2}(b_0 + b_1L^{y_i} + b_2L^{y_{t1}^{(o)}} + b_3L^{y_3} + b_4L^{y_4}) , \quad (13)$$

where  $\chi_a$  and the  $b_i$  are non-universal and depend on the characteristics of the surface;  $\chi_1$  stands for either one of  $\chi_{11}$  and  $\chi_{21}$ . The various parameters in this expression were determined by a least-squares fit. We set  $\chi_a = 0$  to fit  $\chi_{12}$ .

Similarly, we fitted data for the correlation functions  $g_{11}$  and  $g_{12}$  to expressions of the form

$$g_1(L) = L^{2y_{h1}^{(o)}-4}(b_0 + b_1L^{y_i} + b_2L^{y_{t1}^{(o)}} + b_3L^{y_3} + b_4L^{y_4}) , \quad (14)$$

Again,  $g_1$  can be either  $g_{11}$  or  $g_{12}$ ; the non-universal amplitudes  $b_i$  are fitting parameters independent of the corresponding amplitudes in Eq. (13), although we use the same symbols.

The correction terms with amplitudes  $b_1$ ,  $b_2$ ,  $b_3$ , and  $b_4$  in Eqs. (13) and (14) account for the leading finite-size corrections. The exponent  $y_i = -0.821\,(5)$ <sup>24</sup> is the leading irrelevant thermal scaling field in the three-dimensional Ising universality class. Further, since the thermal surface scaling field for the ordinary transition is irrelevant, it may also introduce finite-size corrections. From a simple scaling argument it can be derived that the value of this irrelevant surface exponent is  $y_{t1}^{(o)} = -1$ <sup>47</sup>, independent of the spatial dimensionality.

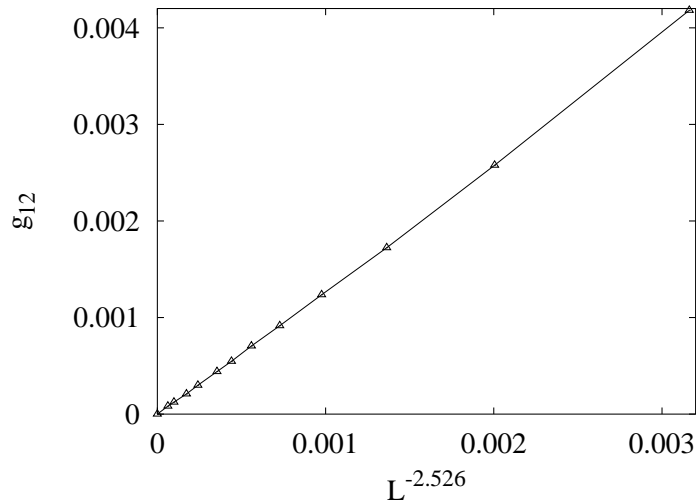


FIG. 2: Surface correlation function  $g_{12}$  vs.  $L^{-2.526}$  for the Ising model with  $\epsilon = 0.8$ . The error margins, in this figure as well as in the following ones, are of the same order as the thickness of the lines.

In principle, finite-size corrections from other sources can occur, so that we also include the terms with amplitudes  $b_3$  and  $b_4$ . We simply took  $y_3 = -2$  and  $y_4 = -3$ .

Separate fits of the  $\chi_{11}$  and  $\chi_{12}$  data, employing Eq. (13), yield consistent estimates:  $y_{h1}^{(o)} = 0.736(2)$  and  $0.738(2)$ , respectively.

Fits of  $g_{11}$  and  $g_{12}$  yield  $y_{h1}^{(o)} = 0.737(2)$  and  $0.736(2)$ , respectively. A joint fit of both sets of susceptibility data, as well as one of both sets of correlation function data, employing a single parameter  $y_{h1}^{(o)}$  and independently variable amplitudes, yielded consistent results but no significant improvement of the accuracy.

We also simulated Ising systems in which the surface enhancement is defined as in Ref. 5. These systems differ from Eq. (1) as to the couplings between the surface layer and the second layer. We thus introduce an enhancement parameter  $\epsilon$  and define couplings  $K_1 = \epsilon^2 K$  between nearest-neighbor sites on the surface, and couplings  $K'_1 = \epsilon K$  between surface sites and their nearest neighbors in next layer. Whenever we parametrize the surface enhancement by  $\epsilon$  we refer to the Hamiltonian defined in Ref. 5, which differs from Eq. (1).

By varying the parameter  $\epsilon$ , one can move closer to the fixed point for the ordinary phase transition so as to reduce the amplitudes of finite-size corrections. Systems with  $\epsilon = 1$  reduce to those described above. In accordance with Ref. 5, in the present work we also

TABLE III: Summary of the results for the surface critical exponents in the three-dimensional Ising model, as obtained by different techniques. MF: mean-field theory, MC: Monte Carlo simulations, FT: field-theoretical methods, CI: Conformal invariance. The MF values of  $y_{t1}$  and  $y_{h1}$  have already made use of the mean-field predictions for the bulk thermal and magnetic exponents, which are  $y_t = 3/2$  and  $y_h = 9/4$ , respectively.

	<i>ordinary</i>		<i>special</i>			
	$y_{h1}$	$\beta_1$	$y_{h1}$	$y_{t1}$	$\beta_1$	$\phi$
MF <sup>1,11</sup>	1/2	1	5/4	3/4	1/2	1/2
MC <sup>18</sup>	0.72 (3)	0.78 (2)	1.71 (16)	0.94 (5)	0.18 (2)	0.59 (4)
MC <sup>20</sup>	0.721 (6)	0.807 (4)	1.623 (3)	—	0.2375 (15)	—
MC <sup>5</sup>	0.740 (15)	—	—	—	—	—
MC <sup>21</sup>	0.73 (1)	0.80 (1)	—	—	—	—
MC+CI <sup>23</sup>	0.737 (5)	0.798 (5)	—	—	—	—
MC <sup>19</sup>	—	—	1.624 (8)	0.73 (2)	0.237 (5)	0.461 (15)
FT <sup>2,15</sup>	0.737	0.796	1.583	0.855	0.263	0.539
FT <sup>16</sup>	0.706	0.816	—	—	—	—
FT <sup>17</sup>	—	—	1.611	1.08	0.245	0.68
Present	0.7374 (15)	0.796 (1)	1.636 (1)	0.715 (1)	0.229 (1)	0.451 (1)

chose  $\epsilon = 0.9$  and  $0.8$ . The analyses of the data for the surface susceptibilities and the correlation functions again employ Eqs. (13) and (14); the results for the surface magnetic exponents are in agreement with those obtained for the case  $\epsilon = 1$ . As an illustration, the data for  $g_{12}$  with  $\epsilon = 0.8$  are shown versus  $L^{2y_{h1}^{(o)}-4}$  in Fig. 2, where  $y_{h1}^{(o)} = 0.737$  is taken from the fit.

Finally, a joint fit to the data for  $\chi_{11}$  and  $\chi_{12}$  for the three cases  $\epsilon = 1.0, 0.9$ , and  $0.8$  yields  $y_{h1}^{(o)} = 0.7374 (15)$ ; this result is in good agreement with most of the existing results, as shown in Table III.

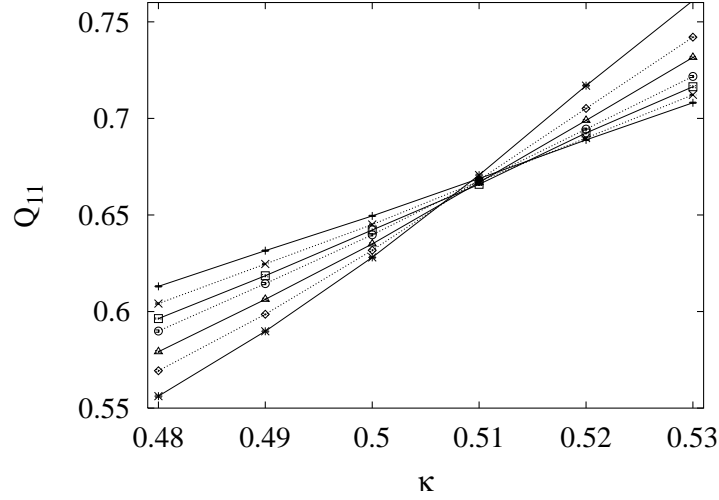


FIG. 3: Surface dimensionless ratio  $Q_{11}$  vs. surface-coupling enhancement  $\kappa$  for the Ising model. The data points  $+$ ,  $\times$ ,  $\square$ ,  $\circ$ ,  $\triangle$ ,  $\diamond$ , and  $*$  represent system sizes  $L = 21, 25, 29, 33, 41, 49$ , and  $63$ , respectively.

### B. Special phase transition

Since it is known that the special transition is located near  $\kappa = (K_1/K) - 1 = 0.5$ , the simulations were performed with surface enhancements  $\kappa$  in the range from 0.46 to 0.54, in steps of 0.01. The system sizes assumed 18 values in the range  $5 \leq L \leq 95$ . We sampled several quantities, including the surface susceptibilities  $\chi_{11}$  and  $\chi_{12}$ , and the universal ratios  $Q_{11}$  and  $Q_{12}$ . Part of the data for  $Q_{11}$  are shown in Fig. 3, in which the clear intersection indicates the location  $\kappa_c^{(s)}$  of the special transition. As mentioned earlier, when  $\kappa$  deviates from  $\kappa_c^{(s)}$ , the finite-size behavior of  $Q_{11}$  is governed by the surface thermal exponent  $y_{t1}^{(s)}$ . We fitted the data for  $Q_{11}$  and  $Q_{12}$  by

$$\begin{aligned}
 Q_1(\kappa, L) = & Q_{1c}^{(s)} + \sum_{k=1}^4 a_k (\kappa - \kappa_c^{(s)})^k L^{ky_{t1}^{(s)}} + \sum_{l=1}^4 b_l L^{y_l} + \\
 & c(\kappa - \kappa_c^{(s)}) L^{y_{t1}^{(s)} + y_i} + n(\kappa - \kappa_c^{(s)})^2 L^{y_{t1}^{(s)}} + r_0 L^{y_a} + \\
 & r_1(\kappa - \kappa_c^{(s)}) L^{y_a} + r_2(\kappa - \kappa_c^{(s)})^2 L^{y_a} + r_3(\kappa - \kappa_c^{(s)})^3 L^{y_a}, \quad (15)
 \end{aligned}$$

where the terms with amplitude  $b_l$  account for various finite-size corrections; and again the subindex 1 in  $Q_1$  and  $Q_{1c}$  is shorthand for 11 or 12, whichever the case may be. The terms with amplitudes  $r_i$  ( $i = 0, \dots, 3$ ) are due to the analytic background. The derivation

of Eq. (15) can be found e.g. in Ref. 24. Naturally, we fixed the exponent  $y_1 = y_i = -0.821(5)^{24}$ , the exponent of the leading irrelevant scaling field in the three-dimensional Ising model. In principle, additional corrections due to irrelevant scaling fields can be induced by the open surfaces, so that we set  $y_2 = y_{i1}$  as an unknown exponent. In order to reduce the residual  $\chi^2$  without discarding data for many small system sizes, we included further finite-size corrections with integer powers  $y_3 = -2$  and  $y_4 = -3$ . The term with coefficient  $n$  reflects the nonlinear dependence of the scaling field on  $\kappa$ , and the one with  $c$  describes the “mixed” effect of the surface thermal field and the irrelevant field. The terms with amplitudes  $r_0$ ,  $r_1$ ,  $r_2$ , and  $r_3$  arise from the analytical part of the free energy, and the exponent  $y_a$  is equal to  $2 - 2y_{h1}^{(s)}$ . As determined later, the surface magnetic exponent at the special transition is about  $y_{h1}^{(s)} = 1.636(1)$ , so that we fixed the exponent  $y_a = -1.272$ . The fits of  $Q_{11}$  yields  $Q_{11c} = 0.626(1)$ ,  $\kappa_c^{(s)} = 0.50214(8)$ , and  $y_{t1}^{(s)} = 0.7154(14)$ ; from the fit of  $Q_{12}$ , we obtain  $Q_{12c} = 0.2689(1)$ ,  $\kappa_c^{(s)} = 0.50207(8)$ , and  $y_{t1}^{(s)} = 0.715(4)$ . Next, we simultaneously fitted the data for  $Q_{11}$  and  $Q_{12}$  by Eq. (15), and obtain  $\kappa_c^{(s)} = 0.50208(5)$ , and  $y_{t1}^{(s)} = 0.715(1)$ . Our estimate  $\kappa_c^{(s)} = 0.50208(5)$  does not agree well with the existing results  $\kappa_c^{(s)} = 0.5004(2)^{19,20}$ . Further, as expected,  $\kappa_c^{(s)}$  does not assume the mean-field value  $1/2$ . Attempts to determine the unknown exponent  $y_{i1}$  and its associated amplitude by least-square fitting to the  $Q_{11}$  and  $Q_{12}$  data were unsuccessful. These corrections, if present, do not exceed the detection threshold. We also fitted the data for the surface susceptibilities  $\chi_{11}$  and  $\chi_{12}$  by

$$\begin{aligned} \chi_1(\kappa, L) = & L^{2y_{h1}^{(s)}-2} [a_0 + \sum_{k=1}^4 a_k (\kappa - \kappa_c^{(s)})^k L^{ky_{t1}^{(s)}} + b_1 L^{y_i} + b_2 L^{y_{i1}} + b_3 L^{y_3} + \\ & b_4 L^{y_4} + c(\kappa - \kappa_c^{(s)}) L^{y_{t1}^{(s)}+y_i} + n(\kappa - \kappa_c^{(s)})^2 L^{y_{t1}^{(s)}} + r_0 L^{y_a} + \\ & r_1 (\kappa - \kappa_c^{(s)}) L^{y_a} + r_2 (\kappa - \kappa_c^{(s)})^2 L^{y_a} + r_3 (\kappa - \kappa_c^{(s)})^3 L^{y_a} + \\ & c_{21} (\kappa - \kappa_c^{(s)}) L^{y_{t1}^{(s)}+y_{i1}} + c_{22} (\kappa - \kappa_c^{(s)})^2 L^{2y_{t1}^{(s)}+y_{i1}}] . \end{aligned} \quad (16)$$

Again, the correction exponents were taken as  $y_i = -0.821(5)^{24}$ ,  $y_3 = -2$ , and  $y_4 = -3$ , and the exponent  $y_2 = y_{i1}$  was left to be fitted. Other than in Eq. (15), we have included in Eq. (16) the combined effect of the surface thermal field and the irrelevant field with the unknown exponent  $y_{i1}$ , as described by the mixed terms with amplitudes  $c_{21}$  and  $c_{22}$ . These terms lead to a reduction of the residual  $\chi^2$  of the fits, but do not significantly modify the result for the surface exponent  $y_{h1}^{(s)}$ . The surface thermal exponent was fixed at  $y_{t1}^{(s)} = 0.715$

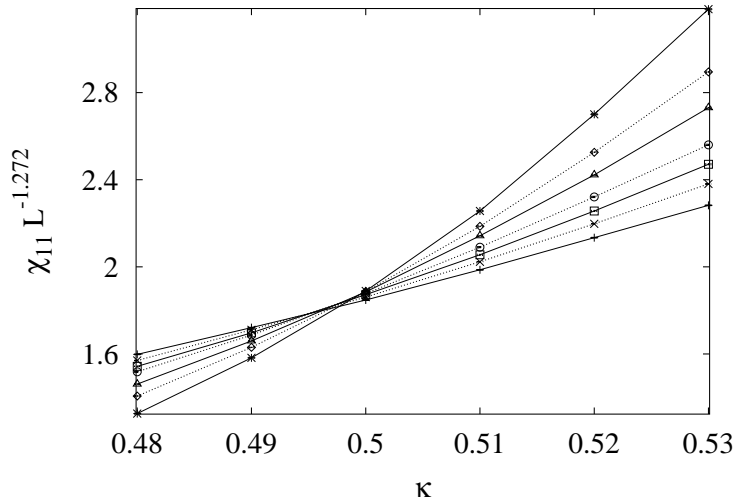


FIG. 4: Surface susceptibility  $\chi_{11} L^{-1.272}$  vs. surface-coupling enhancement  $\kappa$  for the Ising model. The data points  $+$ ,  $\times$ ,  $\square$ ,  $\circ$ ,  $\triangle$ ,  $\diamond$ , and  $*$  represent system sizes  $L = 21, 25, 29, 33, 41, 49$ , and  $63$ , respectively.

as found above. The fit of  $\chi_{11}$  yields  $\kappa_c^{(s)} = 0.50209(9)$ ,  $y_{h1}^{(s)} = 1.636(1)$ , and  $y_{i1} = -0.52(2)$ . The quoted error margins include the uncertainty due to the error in  $y_{t1}^{(s)}$ . In this case we found clear evidence for corrections, introduced by the surfaces with an exponent  $y_{i1}$ . It is remarkable that such corrections are significant only in combination with  $\kappa$ -dependent terms. The data for the surface susceptibility are shown in Fig. 4 as  $\chi_1(\kappa, L)L^{-1.272}$ , where the exponent, which stands for  $2 - 2y_{h1}^{(s)}$ , is chosen such as to suppress the leading  $L$ -dependence at the special transition. As expected, the data display intersections approaching the special transition as determined above.

## V. XY MODEL

The bulk critical point of the XY model was determined as  $K_c = 0.454\,1655(10)$  in Sec. II, which is of sufficient accuracy to perform the following simulations only at this estimated value of  $K_c$ .



### A. Ordinary phase transition

In analogy with the Ising model, we first let the surface couplings  $K_1$  assume the same values of the bulk couplings, i.e.,  $K_1 = K = K_c$ . The system size took 14 values in the range  $4 \leq L \leq 48$ . We sampled the surface susceptibilities  $\chi_{11}$  and  $\chi_{12}$ , and the correlation functions  $g_{11}$  and  $g_{12}$ , and analyzed the data as we did for the Ising model at the ordinary phase transition. For instance, the data for  $\chi_{11}$  and  $\chi_{12}$  were also fitted by Eq. (13), in which the irrelevant exponent was taken as  $y_i = -0.789^{39}$ . The estimates of the surface magnetic exponent  $y_{h1}^{(o)}$  from various quantities agree; the result is  $y_{h1}^{(o)} = 0.781(2)$ .

As a consistency test, in analogy with the Ising model, we also simulated the surface-enhanced  $XY$  model as defined in Ref. 5, with  $\epsilon = 0.9$  and  $0.8$ . As expected, the results for these two cases are in good agreement with the above estimate  $y_{h1}^{(o)} = 0.781(2)$ . However, since the simulations are less extensive in comparison with those for the case  $\epsilon = 1$ , they do not significantly improve the accuracy of  $y_{h1}^{(o)}$ .

### B. Special phase transition

As discussed above, the  $XY$  model is a marginal case in the sense that the line of surface phase transitions for  $K < K_c$  is Kosterlitz-Thouless-like. Still, one would expect that, for  $K = K_c$ , the special and the extraordinary surface transitions occur. Therefore, we performed simulations at the estimated bulk critical point as given above, and varied the surface enhancement from  $\kappa = 0.48$  to  $\kappa = 0.68$ . The system sizes took on 19 values in the range  $5 \leq L \leq 95$ . The sampled quantities include the surface susceptibilities  $\chi_{11}$  and  $\chi_{12}$ , the correlation functions  $g_{11}$  and  $g_{12}$ , and the dimensionless ratios  $Q_{11}$  and  $Q_{12}$ . Part of the data for  $Q_{12}$  are shown in Fig. 5, where the intersection clearly indicates that the special transition occurs near  $\kappa_c = 0.622$ . Further, the increase of the slope of  $Q$  as a function of finite size  $L$  strongly suggests that the surface thermal exponent at  $\kappa_c$  is larger than 0, i.e., that the scaling field associated with  $\kappa$  is not marginal at the special transition. The data for  $Q_{11}$  and  $Q_{12}$  were fitted by Eq. (15), in which the leading irrelevant exponent was fixed at  $y_i = -0.789^{39}$  and the exponent  $y_2 = y_{i1}$  was left free. We obtain  $Q_{11c} = 0.840(1)$ ,  $Q_{12c} = 0.379(2)$ ,  $\kappa_c = 0.6222(3)$ , and  $y_{t1}^{(s)} = 0.608(4)$ . The fits of  $Q_{11}$  and  $Q_{12}$  do not provide clear evidence for the existence of a term with exponent  $y_{i1}$ .

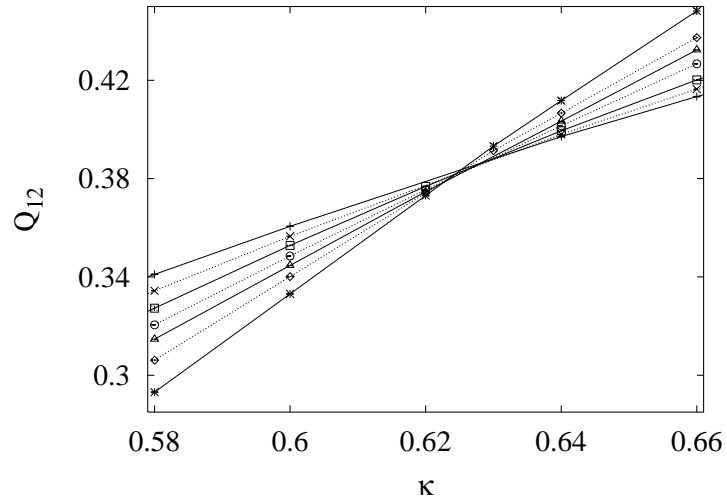


FIG. 5: Surface dimensionless ratio  $Q_{12}$  vs. surface-coupling enhancement  $\kappa$  for the  $XY$  model. The data points  $+$ ,  $\times$ ,  $\square$ ,  $\circ$ ,  $\triangle$ ,  $\diamond$ , and  $*$  represent system sizes  $L = 17, 21, 25, 33, 41, 49$ , and  $63$ , respectively.

TABLE IV: Summary of the results for the surface critical exponents in the three-dimensional  $XY$  and Heisenberg models. MC: Monte Carlo simulations, SE: series expansions.

	<i>ordinary</i>	<i>special</i>	
	$y_{h1}$	$y_{h1}$	$y_{t1}$
MC $(XY)^7$	0.74	—	—
SE $(XY)^{14}$	0.81	—	—
MC $(XY)^5$	0.790 (15)	—	—
Present( $XY$ )	0.781 (2)	1.675 (1)	0.608 (4)
MC (Heisenberg) <sup>5</sup>	0.79 (2)	—	—
Present(Heisenberg)	0.813 (2)	—	—

We also fitted the surface susceptibilities  $\chi_{11}$  and  $\chi_{12}$  by Eq. (16). We obtain the surface magnetic exponent as  $y_{h1}^{(s)} = 1.675(1)$ . Further, we find evidence for new finite-size-corrections with exponent  $y_{i1} = -0.44(4)$ , the major contribution to which comes from the mixed terms with amplitudes  $c_{21}$  and  $c_{22}$  in Eq. (16). Results for the surface exponents are summarized in Table IV.

### C. Extraordinary phase transition

TABLE V: Monte Carlo data for the second moment of surface magnetization  $m_1^2$  and the dimensionless ratio  $Q_{11}$  for the three-dimensional  $XY$  model with enhancement  $\kappa = 1$ .

$L$	7	9	11	13	17	21	25
$m_1^2$	0.5653 (1)	0.5293 (1)	0.5037 (1)	0.4839 (1)	0.4561 (1)	0.4364 (1)	0.4216 (1)
$Q_{11}$	0.96242 (6)	0.96580 (6)	0.96878 (5)	0.97138 (4)	0.97543 (3)	0.97835 (3)	0.98065 (3)
$L$	33	41	49	63	71	81	95
$m_1^2$	0.4004 (1)	0.3859 (1)	0.3747 (1)	0.3601 (1)	0.3540 (1)	0.3473 (1)	0.3397 (1)
$Q_{11}$	0.98381 (3)	0.98601 (3)	0.98748 (3)	0.98927 (3)	0.99004 (3)	0.99085 (3)	0.99169 (3)

Two-dimensional surfaces of the  $XY$  model do not display spontaneous long-ranged surface order for  $K < K_c$ , but they are in a ferromagnetic state in the low-temperature region  $K > K_c$ . Thus the onset of long-range order on the surface also occurs at  $K = K_c$ . This differs from the Ising model, where a long-range ordered surface exists for  $K < K_c$  if  $\kappa > \kappa_c$ . We performed simulations at  $\kappa = 1$  for the critical  $XY$  model with the system sizes in the range  $7 \leq L \leq 95$ . We sampled the second moment of the surface magnetization  $m_1^2$  and the ratio  $Q_{11}$ ; the data for these two quantities are shown in Table V.

In order to analyze the finite-size data in Table V, one first requires the proper scaling formulas. For the extraordinary phase transitions in the  $XY$  model, there exists some ambiguity, because it is not generally clear whether the surfaces undergo a first or a second order transition. Nevertheless, in either case, the surfaces should display some critical singularities, arising from the diverging bulk correlation length. Thus, we fitted the  $m_1^2$  data by

$$m_1^2(L) = m_a^2 + L^{-2X_{h1}^{(e)}} (b_0 + b_1 L^{y_1} + b_2 L^{2y_1}) . \quad (17)$$

If the transition on the surface is first order at  $K = K_c$ , the analytical contribution,  $m_a^2$ , assumes a nonzero value. First, we set the exponent  $y_1 = y_i = -0.789^{39}$ . Satisfactory fits were obtained for all the  $m_1^2$  data in Table V, with the terms  $m_a^2$  and those with  $b_0$  and  $b_1$  only. The results are  $m_a = 0.471 (5)$ ,  $X_{h1}^{(e)} = 0.188 (5)$ ,  $b_0 = 0.65 (1)$ , and  $b_1 = 0.35 (5)$ . The quality of the fit is shown in Fig. 6. Further, we fitted the data for the ratio  $Q_{11}$  by

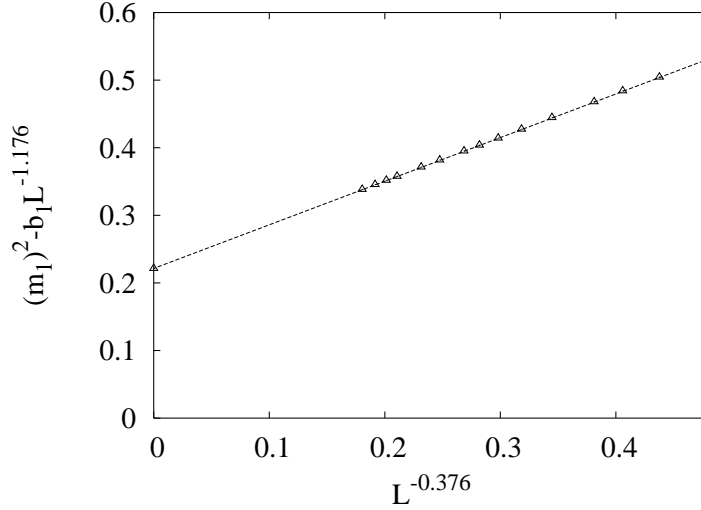


FIG. 6: Surface magnetization in terms of the quantity  $(m_1)^2 - b_1 L^{-1.2}$  vs.  $L^{-2X_{h1}^{(e)}}$  for the  $XY$  model at  $\kappa = 1$ , where the values  $X_{h1}^{(e)} = 0.188(5)$  and  $b_1 = 0.35(5)$  were obtained from a least-squares fit (see text).

$$Q_{11}(L) = Q_c + b_1 L^{-2X_{h1}^{(e)}} + b_2 L^{-2X_{h1}^{(e)} + y_1} + b_3 L^{-2X_{h1}^{(e)} + 2y_1} + b_4 L^{-2X_{h1}^{(e)} + 3y_1}, \quad (18)$$

where the irrelevant exponent is fixed at  $y_1 = y_i = -0.789^{39}$ . The presence of the exponent  $X_{h1}^{(e)}$  is due to the nonzero background contribution  $m_a$  in the second moment of the magnetization  $m_1^2$ . We obtain the asymptotic value  $Q_c = 0.9998(4) \approx 1$ . From the results for  $m_a$  and  $Q_c$ , it seems that the surface transition at  $K = K_c$  and  $\kappa = 1$  is first order. However, it seems also possible that the surface magnetization vanishes only very slowly as the system size  $L$  increases, such that the line of extraordinary transitions on the surfaces is still Kosterlitz-Thouless-like. Thus, we set  $m_a$  in Eq. (17) to zero, and fitted the unknown parameters including both  $X_{h1}^{(e)}$  and  $y_i$  to the  $m_1^2$  data. Indeed, we found that our Monte Carlo data for  $m_1^2$  in Table V can be modeled this way, and we obtain  $b_0 = 0.40(1)$ ,  $b_1 = 0.703(6)$ ,  $X_{h1}^{(e)} = 0.0325(30)$ , and  $y_1 = -0.545(14)$ . This fit is illustrated by Fig. 7. We also fitted the  $Q$  data by Eq. (18) with  $y_1$  fixed at  $-0.545$ , and the result for  $Q_c$  is  $Q_c = 0.9982(15)$ , which is also consistent with 1. In short, our numerical evidence for the surface magnetization of the three-dimensional  $XY$  model is not sufficient to determine whether the line of transitions for  $K = K_c$  and  $\kappa > \kappa_c$  is first or second order, but settling this matter convincingly would require extensive simulations, well beyond the scope of the present investigation.

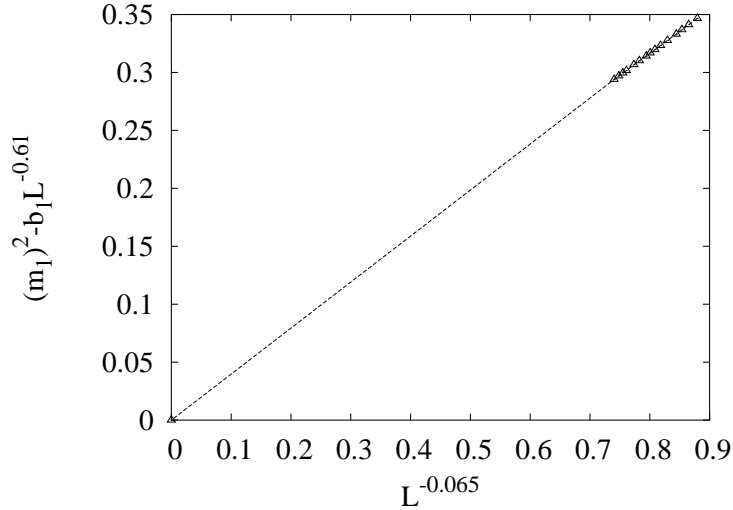


FIG. 7: Surface magnetization in terms of the quantity  $(m_1)^2 - b_1 L^{-0.61}$  vs.  $L^{-0.065}$  for the XY model at  $\kappa = 1$ .

## VI. HEISENBERG MODEL

We simulated the three-dimensional Heisenberg model at  $K_1 = K = K_c = 0.693\,002\,(2)$ , as determined in Sec. II. The system sizes were taken in the range  $4 \leq L \leq 64$ . The data for the surface susceptibilities  $\chi_{11}$  and  $\chi_{12}$ , taken at  $\kappa = 0$ , were fitted by Eq. (13). Using a similar procedure as that for the XY model, we obtain  $y_{h1}^{(o)} = 0.813\,(2)$  for the ordinary phase transition. We also determined the bulk susceptibility  $\chi_b$  and the dimensionless ratios  $Q_{11}$  and  $Q_{12}$  for a range of larger values of the surface enhancement  $\kappa$ . The scaled susceptibility  $\chi_b L^{3-2y_h}$  is shown in Fig. 8. The intersections near  $\kappa \approx 0.8$  are very suggestive of a special transition. The results for  $Q_{11}$ , shown in Figs. 9 and 10, display similar behavior. For  $\kappa \lesssim 0.8$ ,  $Q_{11}$  converges to a universal constant characteristic of the ordinary transition. For  $\kappa \gtrsim 0.8$  the data seem to converge to a  $\kappa$ -dependent value. The overall behavior of the results for  $Q_{11}$  resembles that of the ratio  $Q$  for bulk transitions in the Kosterlitz-Thouless universality class, as reported for the triangular Ising antiferromagnet with nearest- and next-nearest-neighbor interactions<sup>48</sup>. An alternative interpretation would be a special transition with a relevant exponent  $y_{t1}^{(s)}$  only slightly larger than 0. A convincing numerical test of the Kosterlitz-Thouless nature of the special transition would require simulations beyond the scope of the present work.

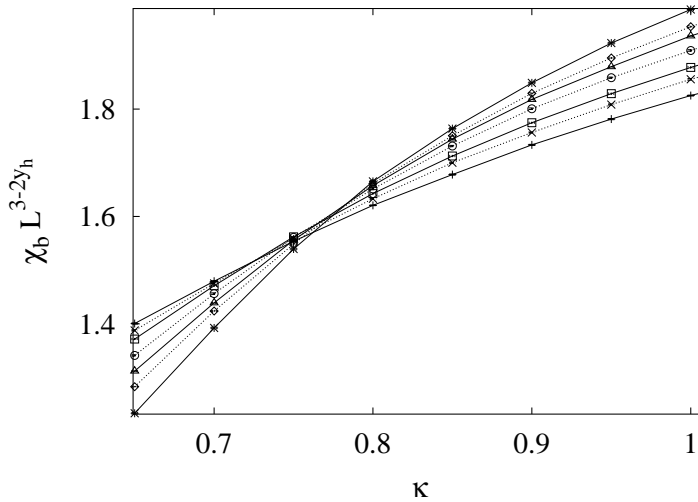


FIG. 8: Critical bulk susceptibility  $\chi_b$  of the Heisenberg model vs. surface enhancement  $\kappa$ . The data shown along the vertical axis are scaled with a size-dependent factor  $L^{3-2y_h}$  where  $y_h = 2.482$  is the bulk magnetic exponent. The data points  $+$ ,  $\times$ ,  $\square$ ,  $\circ$ ,  $\triangle$ ,  $\diamond$ , and  $*$  represent system sizes  $L = 16, 20, 24, 32, 40, 48$ , and  $64$ , respectively. According to the theory, the scaled susceptibility  $\chi_b L^{3-2y_h}$  converges with increasing size  $L$  to a value that may still depend on  $\kappa$ . The intersections near  $\kappa = 0.8$  suggest the existence of a “special” phase transition.

## VII. DISCUSSION

We used Monte Carlo techniques and finite-size scaling in order to obtain new and more accurate results for the bulk and surface critical parameters of the three-dimensional Ising, XY, and Heisenberg models. At the ordinary phase transitions, we determined the surface magnetic exponents as  $y_{h1}^{(o)}(n = 1) = 0.7374(15)$ ,  $y_{h1}^{(o)}(n = 2) = 0.781(2)$ , and  $y_{h1}^{(o)}(n = 3) = 0.813(2)$ . These values are in a satisfactory agreement with earlier results<sup>5</sup>, namely  $y_{h1}^{(o)}(n = 1) = 0.740(15)$ ,  $y_{h1}^{(o)}(n = 2) = 0.790(15)$ , and  $y_{h1}^{(o)}(n = 3) = 0.79(2)$ , as shown in Table IV. Since the bulk thermal exponent  $y_t$  of the  $O(n)$  model decreases with increasing  $n$ , these results suggest that the surface exponent  $y_{h1}^{(o)}$  is a decreasing function of  $y_t$ . The same seems to hold true for the two- and three-dimensional Potts models, as may be concluded on the basis of the following evidence. In three dimensions, the surface magnetic exponent for the  $q \rightarrow 0$  and  $q \rightarrow 1$  Potts models are  $y_{h1}^{(o)} = 2$  and  $1.0246(6)$ <sup>49</sup>, respectively. The former model is generally referred to as the uniform spanning tree<sup>50</sup>, while the  $q \rightarrow 1$  Potts

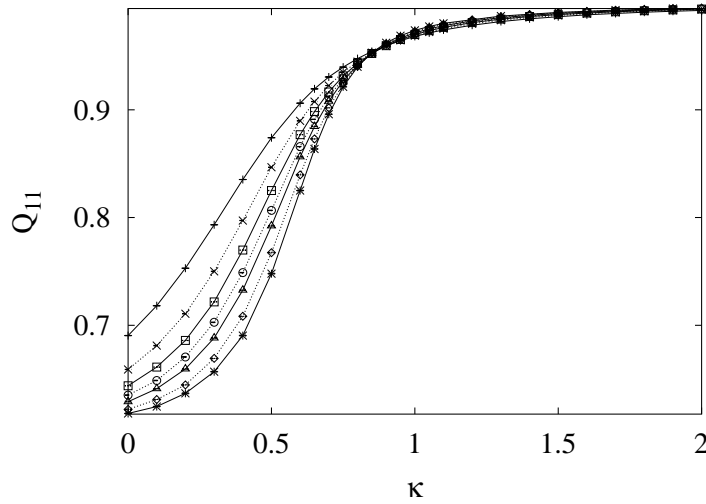


FIG. 9: Surface dimensionless ratio  $Q_{11}$  vs. surface-coupling enhancement  $\kappa$  for the  $O(3)$  model. The data points  $+$ ,  $\times$ ,  $\square$ ,  $\bigcirc$ ,  $\triangle$ ,  $\diamond$ , and  $*$  represent system sizes  $L = 8, 12, 16, 20, 24, 32$ , and  $40$ , respectively. For small surface enhancement  $\kappa \lesssim 0.5$ , the ratio  $Q_{11}$  converges with increasing  $L$  to a nontrivial value near  $0.62$ , just as expected for the ordinary phase transition. For large enhancement  $\kappa > 1$ , it seems that the asymptotic value  $Q_{11}(L \rightarrow \infty)$  is different from  $1$ , and dependent on  $\kappa$ . In the intermediate range  $0.6 < \kappa < 0.9$ , the slope of the  $Q_{11}$  data lines increases with  $L$ . The intersections of these lines seem to converge to a value near  $\kappa = 0.8$ . This figure bears much analogy with that for the bulk ratio  $Q$  of transitions in the Kosterlitz-Thouless universality class.

model reduces to the bond percolation model. For the two-dimensional Potts model, from the conformal field theory, the exponent  $y_{h1}^{(o)}$  is exactly known as  $y_{h1}^{(o)} = 2 - 3/(3 - y_t)^{51}$ , which is a decreasing function of the bulk thermal exponent  $y_t$ . Further, if one applies the above expression to the tricritical branch of the Potts model in two dimensions, one obtains that the surface magnetic scaling field is irrelevant at the ordinary phase transition. Starting from this observation, it was found<sup>8</sup> that rich surface phase transitions can also occur in some two-dimensional systems, although their “surfaces” are just one-dimensional edges.

In the present work, we also located the special transitions of the Ising and the  $XY$  model on the simple-cubic lattice, and obtained numerical estimates of the corresponding renormalization exponents. While the surface transition of the three-dimensional  $XY$  model is Kosterlitz-Thouless-like, and the line of surface transitions connects to the special transition

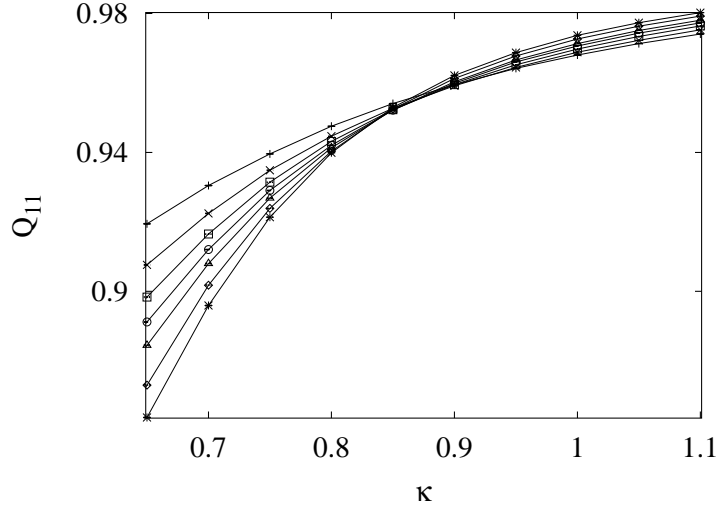


FIG. 10: Surface ratio  $Q_{11}$  in the range  $0.65 \leq \kappa \leq 1.1$  for the O(3) model. The data points  $+$ ,  $\times$ ,  $\square$ ,  $\circ$ ,  $\triangle$ ,  $\diamond$ , and  $*$  represent system sizes  $L = 8, 16, 24, 32, 40, 48$ , and  $64$ , respectively. The apparent convergence of the intersections of the  $Q_{11}$  data with increasing system size indicates a “special” surface transition near  $\kappa = 0.80$ , in agreement with the results in Figs. 8 and 9.

point, our numerical data did not yield evidence for corrections to scaling due to a marginal field at the special transition.

Finally, we note that the surface-critical behavior of the O(1), O(2) and O(3) models is rather dissimilar for large surface enhancements. For the O(1) model, spontaneous surface order exists even below the bulk critical coupling  $K_c$ ; for the O(2) model it exists for  $K > K_c$  and possibly for  $K = K_c$ ; and for the O(3) model only for  $K > K_c$ . In line with the bulk critical singularity, the O( $n$ ) surface critical behavior is thus seen to become less singular with increasing  $n$ . This is also evident from our analyses of the special transitions, which yield relevant exponents  $y_{t1}^{(s)}$  for the O(1) and O(2) models but allow a marginal exponent for the O(3) model. Since the lower critical dimensionality of the special transition<sup>1</sup> is 3 for  $n > 2$ , it seems plausible that the range  $\kappa > \kappa_c$  corresponds with a line of fixed points and  $\kappa$ -dependent critical surface exponents, in agreement with an analysis of the surface magnetization by Krech<sup>9</sup>. Indeed, the data in Figs. 8 and 9 are suggestive of a Kosterlitz-Thouless-like scenario involving a nonuniversal range of  $Q$ -values such as found earlier in the different context of the Ising triangular antiferromagnet<sup>48</sup>.



### Acknowledgments

The authors are indebted to Dr. J.R. Heringa and X.F. Qian for valuable discussions. This research was supported by the Dutch FOM foundation (“Stichting voor Fundamenteel Onderzoek der Materie”) which is financially supported by the NWO (“Nederlandse Organisatie voor Wetenschappelijk Onderzoek”). This research was supported in part by the United States National Science Foundation under grant number ITR 0218858.

- 
- <sup>1</sup> K. Binder, in *Phase Transitions and Critical Phenomena*, edited by C. Domb and J.L. Lebowitz. (Academic, London, 1987), Vol. 8, p. 1, and references therein.
  - <sup>2</sup> H.W. Diehl, in *Phase Transitions and Critical Phenomena*, edited by C. Domb and J.L. Lebowitz. (Academic, London, 1987), Vol. 10, p. 76, and references therein.
  - <sup>3</sup> H.W. Diehl, Int. J. Mod. Phys. B **11**, 3503 (1997).
  - <sup>4</sup> M. Pleimling, J. Phys. A **37**, R79 (2004).
  - <sup>5</sup> M.P. Nightingale and H.W.J. Blöte, Phys. Rev. B **48**, 13 678 (1993).
  - <sup>6</sup> J.M. Kosterlitz and D.J. Thouless, J. Phys. C **5**, L124 (1973).
  - <sup>7</sup> D.P. Landau, R. Pandey, and K. Binder, Phys. Rev. B **39**, 12302 (1989).
  - <sup>8</sup> Y. Deng and H.W.J. Blöte, Phys. Rev. E **70**, 035107(R) (2004).
  - <sup>9</sup> M. Krech, Phys. Rev. B **62**, 6360 (2000).
  - <sup>10</sup> Y. Deng and H.W.J. Blöte, unpublished.
  - <sup>11</sup> K. Binder and P.C. Hohenberg, Phys. Rev. B **6**, 3461 (1972).
  - <sup>12</sup> K. Binder and P.C. Hohenberg, Phys. Rev. B **9**, 2194 (1974).
  - <sup>13</sup> T.C. Lubensky and M.H. Rubin, Phys. Rev. B **12**, 3885 (1975).
  - <sup>14</sup> K. Ohno, Y. Okabe, and A. Morita, Prog. Theor. Phys. **71**, 741 (1984).
  - <sup>15</sup> H.W. Diehl and M. Shpot, Nucl. Phys. B **528**, 595 (1998).
  - <sup>16</sup> H.W. Diehl and S. Dietrich, Z. Phys. B **42**, 65 (1981).
  - <sup>17</sup> H.W. Diehl and S. Dietrich, Phys. Rev. B **24**, R2878 (1981).
  - <sup>18</sup> D.P. Landau and K. Binder, Phys. Rev. B **41**, 4633 (1990).
  - <sup>19</sup> C. Ruge, A. Dunkelmann, F. Wagner, and J. Wulf, J. Stat. Phys. **73**, 293 (1993).
  - <sup>20</sup> C. Ruge and F. Wagner, Phys. Rev. B **52**, 4209 (1995).

- <sup>21</sup> M. Pleimling and W. Selke, Eur. Phys. J. B **1**, 385 (1998).
- <sup>22</sup> K. Binder, D.P. Landau, and M. Muller, J. Stat. Phys. **110**, 1411 (2003).
- <sup>23</sup> Y. Deng and H.W.J. Blöte, Phys. Rev. E **67**, 066116 (2003).
- <sup>24</sup> Y. Deng and H.W.J. Blöte, Phys. Rev. E **68**, 036125 (2003), and references therein.
- <sup>25</sup> M.P. Nightingale, *Finite-Size Scaling and Numerical Simulation of Statistical Systems*, edited by V. Privman (World Scientific, Singapore, 1990), p. 287.
- <sup>26</sup> M.P. Nightingale and H.W.J. Blöte, Phys. Rev. Lett. **60**, 1562 (1988).
- <sup>27</sup> J. Adler, J. Phys. A **16**, 3585 (1983).
- <sup>28</sup> J. Adler, C. Holm, and W. Janke, Physica A **201**, 581 (1993).
- <sup>29</sup> A. Cucchieri, J. Engels, S. Holtmann, T. Mendes, and T. Schulze, J. Phys. A **35**, 6517 (2002).
- <sup>30</sup> H.G. Ballesteros, L.A. Fernández, V. Martín-Mayor, and A.M. Sudupe, Phys. Lett. B **387**, 125 (1996).
- <sup>31</sup> M.E. Fisher and G. Caginalp, Commun. Math. Phys. **56**, 11 (1977).
- <sup>32</sup> G. Caginalp and M.E. Fisher, Commun. Math. Phys. **65**, 247 (1979).
- <sup>33</sup> K. Binder, Z. Phys. B **43**, 119 (1981).
- <sup>34</sup> U. Wolff, Phys. Rev. Lett. **62**, 361 (1989).
- <sup>35</sup> U. Wolff, Phys. Lett. B **228**, 379 (1989).
- <sup>36</sup> A. Hoogland, J. Spaa, B. Selman, and A. Compagner, J. Comp. Phys. **51**, 250 (1983).
- <sup>37</sup> A. Hoogland, A. Compagner and H.W.J. Blöte, in "Architecture and Performance of Specialized Computers" ed. B. Alder, in the series "Computational Techniques",
- <sup>38</sup> L.N. Shchur and H.W.J. Blöte, Phys. Rev. E **55**, R4905 (1997).
- <sup>39</sup> R. Guida and J. Zinn-Justin, J. Phys. A **31**, 8103 (1998).
- <sup>40</sup> W. Janke, Phys. Lett. A **148**, 306 (1990).
- <sup>41</sup> A.P. Gottlob and M. Hasenbusch, Physica A **201**, 593 (1993).
- <sup>42</sup> P. Butera and M. Comi, Phys. Rev. B **56**, 8212 (1997).
- <sup>43</sup> K. Chen, A.M. Ferrenberg, and D.P. Landau, Phys. Rev. B **48**, 3249 (1993).
- <sup>44</sup> C. Holm and W. Janke, Phys. Lett. A **173**, 8 (1993); Phys. Rev. B **48**, 936 (1993). This work has yielded a second estimate of  $K_c$  that is slightly smaller.
- <sup>45</sup> K. Binder and E. Luijten, Phys. Rep. **344**, 179 (2001).
- <sup>46</sup> Y. Deng and H.W.J. Blöte, Phys. Rev. Lett. **88**, 190602 (2002).
- <sup>47</sup> T.W. Burkhardt and J.L. Cardy, J. Phys. A **20**, L233 (1987).

- <sup>48</sup> X.F. Qian and H.W.J. Blöte, Phys. Rev. E **70**, 036112 (2004).
- <sup>49</sup> Y. Deng and H.W.J. Blöte, Phys. Rev. E **71** 016117 (2005).
- <sup>50</sup> for a review, see e.g., F.Y. Wu, Rev. Mod. Phys. **54**, 235 (1982).
- <sup>51</sup> J.L. Cardy, Nucl. Phys. B **240** [FS12], 514 (1984); Nucl. Phys. B **324**, 581 (1989).